

Revisit to non-decoupling MSSM

Jiwei Ke, Hui Luo, Ming-xing Luo, Kai Wang*, Liucheng Wang, Guohuai Zhu

Zhejiang Institute of Modern Physics and Department of Physics, Zhejiang University, Hangzhou, Zhejiang 310027, China

ARTICLE INFO

Article history:

Received 23 November 2012

Received in revised form 22 April 2013

Accepted 26 April 2013

Available online 30 April 2013

Editor: M. Cvetič

ABSTRACT

Dipole operator $\bar{s}\sigma_{\mu\nu}F^{\mu\nu}b$ requires the helicity flip in the involving quark states thus the breaking of chiral $U(3)_Q \times U(3)_d$. On the other hand, the b quark mass generation is also a consequence of chiral $U(3)_Q \times U(3)_d$ symmetry breaking. Therefore, in many models, there might be strong correlation between the $b \rightarrow s\gamma$ and b quark Yukawa coupling. In this Letter, we use non-decoupling MSSM model to illustrate this feature. In the scenario, the light Higgs boson may evade the direct search experiments at LEP II or Tevatron while the 125 GeV Higgs-like boson is identified as the heavy Higgs boson in the spectrum. A light charged Higgs is close to the heavy Higgs boson which is of 125 GeV and its contribution to $b \rightarrow s\gamma$ requires large supersymmetric correction with large PQ and R -symmetry breaking. The large supersymmetric contribution at the same time significantly modifies the b quark Yukawa coupling. With combined flavor constraints $B \rightarrow X_s\gamma$ and $B_s \rightarrow \mu^+\mu^-$ and direct constraints on Higgs properties, we find best fit scenarios with light stop of $\mathcal{O}(500$ GeV), negative A_t around -750 GeV and large μ -term of 2–3 TeV. In addition, reduction in $b\bar{b}$ partial width may also result in large enhancement of $\tau\tau$ decay branching fraction. Large parameter region in the survival space under all bounds may be further constrained by $H \rightarrow \tau\tau$ if no excess of $\tau\tau$ is confirmed at LHC. We only identify a small parameter region with significant $H \rightarrow hh$ decay that is consistent with all bounds and reduced $\tau\tau$ decay branching fraction. In the end, if current dark matter mostly consists of neutralino, direct detection experiments like XENON100 also puts stringent bound over this scenario with light Higgs bosons. The light stops which are required by flavor constraints can further enhance the scattering cross section.

© 2013 Elsevier B.V. All rights reserved.

1. Introduction

A Higgs-like boson of 125 GeV has been discovered at the Large Hadron Collider (LHC) at CERN via two cleanest channels, the di-photon ($gg \rightarrow h \rightarrow \gamma\gamma$) and four-lepton ($gg \rightarrow h \rightarrow ZZ^* \rightarrow \ell_i^+ \ell_i^- \ell_j^+ \ell_j^-$ with $i, j = e^\pm, \mu^\pm$) modes [1]. Later both ATLAS and CMS Collaborations also reported observations in the di-lepton ($gg \rightarrow h \rightarrow WW^* \rightarrow \ell_i^+ \nu_i \ell_j^- \bar{\nu}_j$) channels with the mass range consistent with the four-lepton measurement [2]. However, the confirmation of whether it is the Higgs boson of the standard model (SM) will require comprehensive and precise measurements of Higgs properties. The deviation of the Higgs couplings from the SM ones may imply the existence of the beyond SM physics, in particular, the excess in the di-photon channel with $\sigma_{\text{obs.}}/\sigma_{\text{SM}} \sim 1.5\text{--}2.0$ at both ATLAS and CMS. In all extension theories, additional charged and neutral scalars are inevitable. Therefore, searches of other Higgs-like states also provide direct test to models beyond SM physics. The LHC and Tevatron Collaborations [3] have put stringent bounds over the SM Higgs, particularly

heavy Higgs decaying into pure leptonic final states via WW and ZZ . For instance, CMS Collaboration has excluded the SM Higgs of 110–121.5 GeV and 128–600 GeV at 95% C.L. The LEP II experiments also exclude the SM Higgs with mass lower than 114 GeV via $e^+e^- \rightarrow Zh$ channel. These bounds at the same time apply to various models with Higgs extension.

For two decades, weak scale supersymmetry has been the most elegant candidate to cancel the quadratic divergence if the Higgs boson is indeed a fundamental scalar. Within the supersymmetric framework, there exist several scenarios where the di-photon decay branching fraction is enhanced, for instance, models with light stau [4] or light stop [5]. Another particularly interesting region of non-decoupling limit in minimal supersymmetric standard model (MSSM) has been discussed by various authors [6–14]. It was observed that there might exist even lighter Higgs h which evades the search at LEP [6] due to suppressed ZZh coupling and thus production of Zh . The light Higgs h can then have $M_h < m_Z$ while the Higgs-like boson of 125 GeV can be identified as the heavier degree of freedom H . To reduce the ZZh coupling $g_{ZZh} = \sin(\beta - \alpha)$ which is the vacuum expectation value (v_{ev}) of h , simple realization is to let h be the H_d -like boson since large m_t naturally requires large v_u . Given h is a mixture state as $-\sin\alpha(\text{Re } H_d) + \cos\alpha(\text{Re } H_u)$, this scenario prefers $\sin\alpha \simeq -1$ and

* Corresponding author.

E-mail address: wangkai1@zju.edu.cn (K. Wang).

large $\tan\beta$ which suppresses the v_d . In the limit of large $\tan\beta$ as $\sin\beta \rightarrow 1$, $\sin\alpha \rightarrow -1$ gives the $\sin(\beta - \alpha)$ approaches zero. On the other hand, within MSSM, at tree level, the Higgs mass matrix gives

$$\frac{\tan 2\alpha}{\tan 2\beta} = \frac{M_A^2 + m_Z^2}{M_A^2 - m_Z^2}. \quad (1)$$

Taking $M_A \rightarrow 0$ and the $\beta \rightarrow \pi/2$ as limit of large $\tan\beta$, one can get $\alpha \rightarrow -\pi/2$ which results in $\sin(\beta - \alpha) \rightarrow 0$ and reproduce the previous requirement. For $M_A \gtrsim 200$ GeV, the g_{ZZh} goes to the SM value. However, since the charged Higgs state H^\pm are at the similar scale as M_H as $M_{H^\pm}^2 = M_A^2 + m_W^2$ at tree level, small M_A leads to lighter H^\pm which suffers from direct search bounds of light charged Higgs. Drell-Yan production of charged Higgs pair at LEP $e^+e^- \rightarrow H^+H^-$ put strict bounds as $M_{H^\pm} > 80\text{--}100$ GeV depends on its decay [15]. Combining all the constraints, one expect an intermediate M_A region around m_Z scale to be consistent with the LEP II Zbb search and charged Higgs search at LEP, Tevatron and LHC. In the limit of $M_A \rightarrow m_Z$, h and H masses at tree level are degenerate which is known as non-decoupling limit.

By requiring M_H to be at 125 GeV, the first consequence of these non-decoupling scenarios is that the charged Higgs is around similar scale. Charged scalar below top quark mass receives stringent bound from the ATLAS search of $t \rightarrow bH^+$ with $H^+ \rightarrow \tau^+\nu$ requires the $\text{BR}(t \rightarrow bH^+) \times \text{BR}(H^+ \rightarrow \tau^+\nu_\tau) < 1\text{--}5\%$ for mass range M_{H^\pm} in between 90 and 160 GeV [16]. In the conventional Two-Higgs-Doublet models (2HDM) such a light charged Higgs suffer severe constraints due to flavor violation processes [17]. For example, one might be concerned by $B_u \rightarrow \tau\nu_\tau$ and $B \rightarrow D^{(*)}\tau\nu_\tau$ decays which receive charged Higgs contributions at the tree level. The two most sensitive parameters involved in Higgs interaction are M_A and $\tan\beta$. As we argued, M_A is taken to be not much heavier than m_Z and LEP2 Zh search prefers a relatively large $\tan\beta$. In addition, as we will show later, the recent search of $t \rightarrow bH^+$ at the LHC restricts $\tan\beta \sim 10$ in non-decoupling region. For $B_u \rightarrow \tau\nu_\tau$ decay, the W^\pm -mediated SM contribution is helicity suppressed. Therefore, even though the charged scalar is somewhat heavier, its contribution could be comparable to the SM part if $\tan\beta$ is not small [18–20]:

$$\frac{\text{BR}(B^+ \rightarrow \tau^+\nu)_{\text{MSSM}}}{\text{BR}(B^+ \rightarrow \tau^+\nu)_{\text{SM}}} \simeq \left(1 - \frac{m_B^2}{M_{H^\pm}^2} \tan^2\beta\right)^2 \quad (2)$$

where the MSSM corrections to the down quark and lepton mass matrix have been neglected, which is safe for $\tan\beta \sim 10$. For M_{H^\pm} lies around 120–150 GeV, the MSSM prediction would be about 20–30% smaller than the SM result of $(0.95 \pm 0.27) \times 10^{-4}$. While the experimental world average is $(1.65 \pm 0.34) \times 10^{-4}$ before 2012 [21], Belle updated their measurement at ICHEP2012 with much smaller value $0.72_{-0.27}^{+0.29} \times 10^{-4}$ for hadronic tag of τ [22]. So in the non-decoupling limit, a light charged Higgs with $\tan\beta \sim 10$ is well consistent with the new Belle measurement. Similarly, the charged Higgs contribution to $B \rightarrow D^{(*)}\tau\nu_\tau$ decays are not very significant in the interesting region of M_{H^\pm} and $\tan\beta$. Therefore we will not discuss the bounds from $B^+ \rightarrow \tau^+\nu$ and $B \rightarrow D^{(*)}\tau\nu_\tau$ decays further in our study.

On the other hand, the penguin $b \rightarrow s$ processes are also sensitive to the charged Higgs effects. Generally, $b \rightarrow s\gamma$ and $B_s \rightarrow \mu^+\mu^-$ are two most stringent constraints. But choosing appropriate MSSM parameters, supersymmetric contributions may cancel part of the SM and charged Higgs amplitudes [23]. For example, $b \rightarrow s$ transition mediated by the scalar top quark (stop) loop in MSSM may cancel the top quark loop in SM and 2HDM in some parameter region. One can thus expect that light stop in MSSM

may significantly reduce the flavor violation [24]. In this Letter, we start with this argument and study whether scenarios with light stop can resolve the tension in flavor physics due to the light charged Higgs H^\pm .

Search of $\mu \rightarrow e\gamma$ at the MEG experiment will soon reach $\text{BR}(\mu \rightarrow e\gamma) \simeq 1 \times 10^{-13}$. The one loop contribution from charged state to $\mu \rightarrow e\gamma$ is suppressed by small lepton masses and additional helicity flip. The largest contribution in Higgs mediated $\mu \rightarrow e\gamma$ is usually the Barr-Zee two-loop effects involving the charged scalar coupling to a top-bottom loop. However, [25] shown that the charged Higgs contribution only reaches the sensitivity for $\tan\beta$ of 60 for M_A of 100 GeV where the $\tan\beta$ is much larger than what is considered in non-decoupling scenarios.

With conserved R -parity, the thermal relic abundance of the lightest neutralino (LSP) can often be identified with dark matter (DM), consistent with the current cosmological observations. In recent years, direct detection of weakly interacting (WIMP) DM particle through the DM scattering with nuclei has excluded large parameter space of supersymmetric DM and put stringent bound on many models. The latest bound from XENON100 is about 5×10^{-9} pb for DM mass around 200 GeV [26]. Neutral Higgs states h, H can also mediate the scattering between DM and nuclei which is of $1/M_{h,H}^4$. Then the second consequence of non-decoupling scenarios is that the spin-independent scattering is significantly enhanced by the interaction through neutral Higgs H, A of $\mathcal{O}(100)$ GeV [27]. Therefore, models with only neutralino DM in the non-decoupling MSSM suffer stringent constraints from direct detection experiments. In addition, light stop which may significantly improve the flavor physics behavior of non-decoupling MSSM as argued above, would further enhance the scattering of DM and nuclei and put stronger bound on non-decoupling scenarios with only neutralino DM.¹

In the next section, we discuss some general constraints on the non-decoupling scenarios and the scan results. Then we discuss in details the physics interpretation of the scan results, in particular, light stop contribution to cancel light charged Higgs and its implication to M_H , di-photon, di-tau decay and the direct detection experiments of neutralino dark matter. We then conclude in the final section.

2. General constraints and their implications

In this section, we first scan the parameter space with focus on non-decoupling region with M_A is at $\mathcal{O}(m_Z)$ then discuss in details the physics interpretation of scan results.

Latest data from the LHC require the resonance to be at 125 GeV with di-photon decay enhanced with respect to the SM prediction. We therefore impose the selection rules as

- $M_H: 125 \pm 2$ GeV;
- $R_{\gamma\gamma} = \sigma_{\text{obs}}^{\gamma\gamma} / \sigma_{\text{SM}}^{\gamma\gamma}: 1\text{--}2$;
- Combined direct search bounds from HiggsBound3.8.0;
- $\text{BR}(B \rightarrow X_s\gamma) < 5.5 \times 10^{-4}$;
- $\text{BR}(B_s \rightarrow \mu^+\mu^-) < 6 \times 10^{-9}$.

Without loss of generality, we fix masses of the following sfermions as

$$M_{\tilde{Q}_{1,2}} = M_{\tilde{u}_{1,2}} = M_{\tilde{d}_{1,2,3}} = M_{\tilde{L}_{1,2,3}} = M_{\tilde{e}_{1,2,3}} = 1 \text{ TeV}, \quad (3)$$

and the gauginos as

¹ If the DM is not dominated by the neutralino component, the bound can be evaded.

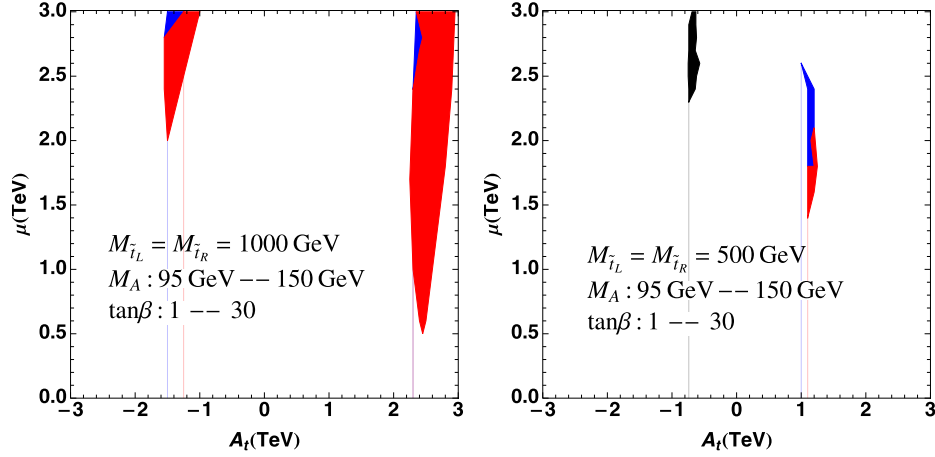


Fig. 1. Scan results in $[A_t, \mu]$ plane. The heavy (light) stop scenario with $M_{\tilde{Q}_3} = M_{\tilde{t}} = 1$ (0.5) TeV is shown in the left (right) plot. The red region pass the direct search bounds from HiggsBounds with a heavy CP-even Higgs $M_H = 125 \pm 2$ GeV and an enhanced di-photon rate $1 < R_{\gamma\gamma} < 2$. The blue region pass in addition the constraint of $\text{BR}(B \rightarrow X_s \gamma)$, while the black region pass all the constraints, including further the restriction of $\text{BR}(B_s \rightarrow \mu^+ \mu^-)$. (For interpretation of the references to color in this figure legend, the reader is referred to the web version of this Letter.)

$$M_1 = 200 \text{ GeV}, \quad M_2 = 400 \text{ GeV}, \quad M_3 = 1200 \text{ GeV}. \quad (4)$$

As argued, our study focus on the flavor constraints of the non-decoupling MSSM and $b \rightarrow s$ transitions like $B \rightarrow X_s \gamma$ and $B_s \rightarrow \mu^+ \mu^-$ provide the most severe constraints. Light stop usually helps to cancel the charged Higgs contribution in $b \rightarrow s$ transition. On the other hand, for light stop below 500 GeV, we find that the gluon fusion production of H is suppressed significantly with respect to the SM value due to the cancellation between top squark and top quark in the loop. Thus, for light stop ($M_{\tilde{t}} < 500$ GeV), it is difficult to achieve enhanced di-photon. For comparison, we take the third generation up quark masses as

$$M_{\tilde{Q}_3} = M_{\tilde{t}} = 500 \text{ GeV} \quad \text{and a second group with 1 TeV}. \quad (5)$$

We do the scan over four parameters²

$$M_A: 95\text{--}150 \text{ GeV},$$

$$\tan \beta: 1\text{--}30,$$

$$\mu: 200 \text{ GeV--}3 \text{ TeV},$$

$$A_u = A_d = A_t: -3\text{--}3 \text{ TeV}. \quad (6)$$

Discussed by many authors [4], light stau states may significantly enhance the di-photon rate of the Higgs-like boson decay which are observed by both ATLAS and CMS Collaborations. On the other hand, we don't require much stronger di-photon bound as $R_{\gamma\gamma}$ to be the experimental preferred central value of 1.5. Stau states are irrelevant to the flavor constraints from $b \rightarrow s$ transition but only give minor change to the Higgs boson mass. Therefore, we don't take light stau in the study.

We use *FeynHiggs* 2.9.2 [28]³ with *HiggsBounds* 3.8.0 [29] and *SUSY_Flavor* 2.01 [30] to perform the scan here. Fig. 1 shows the scan results in 2D-plot of A_t and μ . M_A and $\tan \beta$ are also varied but aren't shown in the figures. Fig. 1(a) is the heavy stop scenario with $M_{\tilde{Q}_3} = M_{\tilde{t}} = 1$ TeV and (b) is the light stop scenario with $M_{\tilde{Q}_3} = M_{\tilde{t}} = 500$ GeV. Points in red region pass the direct search bounds from HiggsBounds with a heavy CP-even

Higgs $M_H = 125 \pm 2$ GeV and an enhanced di-photon rate $1 < R_{\gamma\gamma} < 2$. The points in blue region pass in addition the constraint of $\text{BR}(B \rightarrow X_s \gamma)$, while the points in black region pass all the constraints, including further the restriction of $\text{BR}(B_s \rightarrow \mu^+ \mu^-)$.

The scenario with heavy stop can survive the $B \rightarrow X_s \gamma$ constraints. However, none of the scanned points can pass the $B_s \rightarrow \mu^+ \mu^-$. In the case of light stop of 500 GeV, we find a small survival parameter region with negative A_t around 750 GeV and large μ -term between 2 and 3 TeV. In the following subsections, we discuss in details the physics implications of the scanned results.

2.1. $b \rightarrow s \gamma$ and $B_s \rightarrow \mu^+ \mu^-$

$b \rightarrow s \gamma$ and $B_s \rightarrow \mu^+ \mu^-$ turn out to be the most stringent flavor physics bounds in the non-decoupling limit. The helicity for the involved quark states must be flipped in $b \rightarrow s \gamma$. Hence, both chiral symmetry $U(3)_Q \times U(3)_d$ and electroweak symmetry $SU(2)_L \times U(1)_Y$ must be broken. The SM $b \rightarrow s$ transition is mediated by the charged weak boson W^- and only left-handed quarks are involved in the weak interaction. Consequently, $b \rightarrow s \gamma$ is suppressed by mass insertion of bottom quark mass m_b in the SM. In MSSM, the charged Higgs H^- -top quark loop contribution to $b \rightarrow s \gamma$ is also suppressed by m_b insertion, and has the same sign as the SM amplitude. Besides the above contributions, squarks can also generate $b \rightarrow s \gamma$ in MSSM which may not flip the helicity of the involved quark states, for instance, loops with right-handed stop-Higgsino ($\tilde{t}_R - \tilde{H}_u$) or left-handed stop-Wino ($\tilde{t}_L - \tilde{W}$). Therefore the squark contributions, in particular the top squark ones, are not necessarily suppressed by m_b , which is helpful to cancel the SM and charged Higgs amplitudes with appropriate MSSM parameters. Consequently, scalar top quark with small $M_{\tilde{t}}$, say ~ 500 GeV, could significantly reduce $b \rightarrow s$ transition.

The squark contributions can be decomposed into chargino penguins, wino penguins and gluino penguins. Chargino penguins contain $\tan \beta$ -enhanced term which arises from v_u insertion in $Q d^c (H_u^*)$. The term explicitly breaks Peccei-Quinn symmetry as well as R -symmetry and is proportional to μA_t . This contribution would destructively interfere with the SM and charged Higgs amplitudes in case of $\mu A_t < 0$ [31,32]. In our study, gluino penguins are also important as they contain terms enhanced by $\mu \tan \beta$ and terms chirally enhanced by $m_{\tilde{g}}/m_b$. Numerically, we use the *FeynHiggs* program to get the non-MFV result of $\text{BR}(B \rightarrow X_s \gamma)$. The experimental world average of this process is $(3.43 \pm 0.22) \times 10^{-4}$

² We confine ourselves to $M_A \lesssim 150$ GeV for larger splitting between h and H which can reduce the $\tau \tau$ decay branching ratio. Details is discussed later.

³ In this scan, we take the pole mass of m_t instead of the running m_t mass. The survival parameter region after scan may be shifted by a few percent.

[21], while the SM prediction up to NNLO perturbative QCD corrections is $(3.15 \pm 0.23) \times 10^{-4}$ [33]. However, $B \rightarrow X_s \gamma$ decay is evaluated only at NLO in the FeynHiggs program, which produces the SM result as 3.8×10^{-4} . This is about 30% larger than the NNLO SM prediction. Taking this and the theoretical and experimental uncertainties into account, we require loosely $\text{BR}(B \rightarrow X_s \gamma)_{\text{MSSM}} < 5.5 \times 10^{-4}$ as the selection rule in the scan.

In the SM, $\text{BR}(B_s \rightarrow \mu^+ \mu^-)$ is strongly helicity suppressed by the small muon mass as $m_\mu^2/m_{B_s}^2$, which leads to a tiny branching ratio of $(3.27 \pm 0.23) \times 10^{-9}$ [34]. However, it is well known that the MSSM contributions to this decay could be enhanced several orders of magnitude larger than the SM prediction in large $\tan\beta$ limit, as the leading contribution of Higgs penguin diagrams to the branching ratio are proportional to $\tan^6\beta$. In our study, $\tan\beta \sim 10$ is not very large, so all the 1-loop diagrams have to be considered, including the charged Higgs diagrams which is enhanced up to $\tan^2\beta$ at the amplitude level. Notice that $B_s \rightarrow \mu^+ \mu^-$ decay is even more sensitive to the MSSM parameters in the non-decoupling limit as the neutral Higgs bosons are all light. Experimentally, a combined search of ATLAS, CMS and LHCb has set the upper limit of 4.2×10^{-9} [35] for time integrated branching ratio. As pointed out in [36,37], this upper limit should be reduced by about 10% when compared with the theoretical calculation. Numerically, we use the SUSY_FLAVOR program [30] to get the complete NLO result of $\text{BR}(B_s \rightarrow \mu^+ \mu^-)$. However, we notice that SUSY_FLAVOR evaluates this branching ratio to be 4.8×10^{-9} in the SM. This is about 50% larger than the SM prediction of $(3.27 \pm 0.23) \times 10^{-9}$ in [34], probably mainly due to different choice of hadronic parameters. Taking this into account, we set the corresponding selection rule to be $\text{BR}(B_s \rightarrow \mu^+ \mu^-)_{\text{MSSM}} < 6 \times 10^{-9}$ in the scan.

In Fig. 1, the black region which satisfy all the constraints give $10^4 \text{BR}(B \rightarrow X_s \gamma)_{\text{MSSM}}$ in the region [4.9, 5.3] and $10^9 \text{BR}(B_s \rightarrow \mu^+ \mu^-)_{\text{MSSM}}$ in the region [2.3, 4.3]. Notice that $\text{BR}(B \rightarrow X_s \gamma)$ is always larger than the SM prediction, which is mainly due to the enhancement of light charged Higgs. For $\text{BR}(B_s \rightarrow \mu^+ \mu^-)$, it is always somewhat smaller than the SM prediction.

2.2. Higgs mass and its decay properties

We discuss the mass spectrum of the Higgs bosons in non-decoupling MSSM and its decay properties in this section. More general discussion can be found in [38]. In particular, we focus on the parameter region that minimizes the flavor violation in $b \rightarrow s$ transition. Combined constraints from $B \rightarrow X_s \gamma$ and $B_s \rightarrow \mu^+ \mu^-$, we take light stop of $M_{\tilde{t}} \sim 500$ GeV with negative A_t of $\mathcal{O}(-750)$ GeV and large μ -term of 2–3 TeV. MSSM contains two $SU(2)_L$ doublets H_u and H_d with the ratio of their vevs $\tan\beta = v_u/v_d$. To evade LEP II bounds, non-decoupling limit corresponds to a region of much lighter H_d state with small v_{ev} in the spectrum. After spontaneously electroweak symmetry breaking, MSSM gives rise to five physical states of Higgs bosons, the two CP-even scalar h, H with one CP odd scalar state A and charged scalars H^\pm . The two CP-even scalar bosons h, H arise from mixing of the real gauge eigenstates ($\text{Re } H_d, \text{Re } H_u$),

$$\begin{pmatrix} h \\ H \end{pmatrix} = \begin{pmatrix} -\sin\alpha & \cos\alpha \\ \cos\alpha & \sin\alpha \end{pmatrix} \begin{pmatrix} \text{Re } H_d \\ \text{Re } H_u \end{pmatrix}. \quad (7)$$

After diagonalizing the general mass matrix of neutral Higgs

$$\mathcal{M}^2 = \begin{pmatrix} \mathcal{M}_{11}^2 & \mathcal{M}_{12}^2 \\ \mathcal{M}_{21}^2 & \mathcal{M}_{22}^2 \end{pmatrix}, \quad (8)$$

the masses of two CP-even Higgs are

$$\begin{cases} M_h^2 = \mathcal{M}_{11}^2 \sin^2\alpha + \mathcal{M}_{22}^2 \cos^2\alpha - \mathcal{M}_{12}^2 \sin 2\alpha, \\ M_H^2 = \mathcal{M}_{11}^2 \cos^2\alpha + \mathcal{M}_{22}^2 \sin^2\alpha + \mathcal{M}_{12}^2 \sin 2\alpha. \end{cases} \quad (9)$$

To illustrate the feature, we take the limit of $\sin(\beta - \alpha) \rightarrow 0$ which is the vanishing limit of g_{ZZh} to completely suppress the Zh production at LEP II. As a result of $\sin\alpha \rightarrow -1$ and $\sin\beta \rightarrow 1$, we have

$$\begin{cases} M_h \simeq \mathcal{M}_{11}, \\ M_H \simeq \mathcal{M}_{22}. \end{cases} \quad (10)$$

Radiative corrections to the elements in mass matrix Eq. 9 are given in [39]. We list the most relevant \mathcal{M}_{22} in Eq. 11

$$\begin{aligned} M_H^2 &\simeq \mathcal{M}_{22}^2 \\ &\simeq M_A^2 \cos^2\beta + m_Z^2 \sin^2\beta \left(1 - \frac{3}{8\pi^2} y_t^2 t \right) \\ &\quad + \frac{y_t^4 v^2}{16\pi^2} 12 \sin^2\beta \left\{ t \left[1 + \frac{t}{16\pi^2} (1.5y_t^2 + 0.5y_b^2 - 8g_3^2) \right] \right. \\ &\quad + \frac{A_t \bar{a}}{M_{\text{SUSY}}^2} \left(1 - \frac{A_t \bar{a}}{12M_{\text{SUSY}}^2} \right) \left[1 + \frac{t}{16\pi^2} (3y_t^2 + y_b^2 - 16g_3^2) \right] \left. \right\} \\ &\quad - \frac{v^2 y_b^4}{16\pi^2} \sin^2\beta \frac{\mu^4}{M_{\text{SUSY}}^4} \left[1 + \frac{t}{16\pi^2} (9y_b^2 - 5y_t^2 - 16g_3^2) \right] \\ &\quad + \mathcal{O}(y_t^2 m_Z^2) \end{aligned} \quad (11)$$

where g_3 is the QCD running coupling constant, y_t and y_b are the top and bottom Yukawa couplings. M_{SUSY} is the arithmetic mean of top squark masses $M_{\tilde{t}}$. A_t is the SUSY breaking A -term associated with top squark and μ is the Higgsino mass parameter. t is defined as $\ln(M_{\text{SUSY}}^2/m_t^2)$ and

$$\bar{a} \equiv A_t - \mu/\tan\beta. \quad (12)$$

In Eq. (11), only the leading terms in powers of y_b and $\tan\beta$ have been retained. Even though the Eq. (11) is only valid in the limit of small splittings between the running stop masses, it shows the qualitative feature for how couplings to stop and sbottom modify the Higgs masses. M_A is $\cos\beta$ dependent which is suppressed in the limit of large $\tan\beta$. Therefore, the M_H is not very sensitive to M_A and with $\tan\beta \simeq 10$, varying M_A by 100 GeV results in 10 GeV difference in M_H . Unlike the m_h^{max} scenario with $\bar{a} = \sqrt{6}M_{\text{SUSY}}$ which is usually used in many studies, minimization of the flavor violating $b \rightarrow s$ transition leads to our best fit parameter region around

$$A_t \sim -750 \text{ GeV}, \quad M_{\tilde{t}} \sim 500 \text{ GeV}, \quad \mu \sim 2000\text{--}3000 \text{ GeV}. \quad (13)$$

The particular choices of A_t and $M_{\tilde{t}}$ significantly modifies the Higgs boson masses through radiative corrections. In our studies, we use the FeynHiggs program to compute the mass spectrum of Higgs in which full radiative corrections of Higgs masses have been implemented [28]. Fig. 2 shows how the M_{h,H,H^\pm} vary with respect to M_A for one of our benchmark points $\tan\beta = 11$, $M_{\tilde{t}} = 500$ GeV, $A_t = -740$ GeV and $\mu = 2300$ GeV. For a large range of M_A , M_H is around 125 GeV. Non-decoupling limit of nearly degenerate h, H lies near $M_A \sim 160$ GeV.

Since H is mostly H_u with large $\tan\beta$, the v_u dominates the electroweak symmetry breaking v . The couplings between H and W^+W^- and top quark t are similar to their SM values. Since the di-photon decay is dominated by the W -boson contribution, the di-photon decay partial width is not changed significantly from the SM $\Gamma_{\text{SM}}(H \rightarrow \gamma\gamma)$. However, di-photon decay branching fraction $\text{BR}(H \rightarrow \gamma\gamma)$ may still be enhanced due to decrease of H

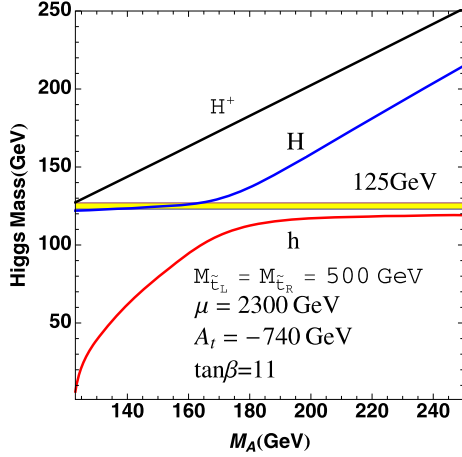


Fig. 2. M_{h,H,H^\pm} vary with respect to M_A for $M_{\tilde{t}} = 500$ GeV, $A_t = -740$ GeV, $\tan\beta = 11$, $\mu = 2300$ GeV.

total width. At 125 GeV, $H \rightarrow b\bar{b}$ and $H \rightarrow WW^*$, $H \rightarrow ZZ^*$ dominate the H decay. Since H is mostly H_u -like, H coupling to b is naturally suppressed. Given $v_u \sim v$, g_{HZZ} and g_{HWW} are not significantly changed from the SM g_{hZZ}^{SM} and g_{hWW}^{SM} . The partial widths of $H \rightarrow WW^*$ and $H \rightarrow ZZ^*$ are indifferent from the SM values. With the reduction in $H \rightarrow b\bar{b}$, the increase of $H \rightarrow WW^*$ and $H \rightarrow ZZ^*$ are inevitable. Therefore, light stau states in the spectrum can improve the di-photon behavior $R_{\gamma\gamma}$ and reduce the tension in increasing ZZ^* or WW^* .

Discussed in [10], in the non-decoupling limit when $H \rightarrow b\bar{b}$ still dominates the H decay, $H \rightarrow \tau^+\tau^-$ can be significantly enhanced.

$$R_{\tau\tau} \simeq r_{gg} \left(\frac{1 + \Delta_b}{1 + \Delta_b(1 - \epsilon)} \right)^2 \quad (14)$$

where $\epsilon = 1 + \tan\alpha/\tan\beta$ with $\alpha < 0$, Δ_b is from the radiative correction in bottom Yukawa, r_{gg} is the ratio in gluon fusion production of H which is order 1 in relatively large $\tan\beta$ and $M_{\tilde{t}} > 500$ GeV. With the radiative correction, $Hb\bar{b}$ coupling is

$$g_{Hb\bar{b}} = \frac{\cos\alpha}{\cos\beta} \left[1 - \frac{\Delta_b}{1 + \Delta_b} \left(1 - \frac{\tan\alpha}{\tan\beta} \right) \right]. \quad (15)$$

Similar to the story of μA_t in $b \rightarrow s$ transition, Δ_b also breaks Peccei-Quinn symmetry and R -symmetry at the same time. In this case, Δ_b contains two R -symmetry breaking pieces as gluino mass $M_{\tilde{g}}$ and A -term contribution. Our choice of $\mu A_t < 0$ results in cancellation between the two contribution but the enhancement to $R_{\tau\tau}$ is still significant. Our results also confirm the finding in [10] with many points of enhanced $H \rightarrow \tau\tau$ decay. Fig. 3 shows the correlation between $\text{BR}(H \rightarrow \tau^+\tau^-)$ and $\text{BR}(H \rightarrow b\bar{b})$ in the survival points. On the other hand, we also find many points with $R_{\tau\tau} < 1$. One particularly interesting feature around non-decoupling limit is that $H \rightarrow hh$ decay may open up and take significant portion of the H decay. In large parameter region, $H \rightarrow hh$ decay partial width may completely dominate the decay of H once it opens up. Discussed in [41], the tree level $H \rightarrow hh$ decay and one loop contributions may have different signs and severely cancel each other.⁴ There then exists a very fine tuned parameter region that the $\Gamma(H \rightarrow hh)$ is at similar order as other decay and only takes about 50% of H decay. If $H \rightarrow hh$ decay occurs, h can further decay into $b\bar{b}$ or $\tau\tau$, the search of H then fall

⁴ The result is based on full one loop calculation in [41] and stability of the result may require higher order calculation.

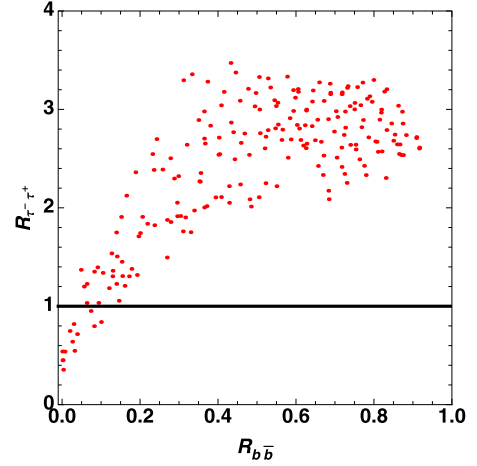


Fig. 3. $\text{BR}(H \rightarrow \tau^+\tau^-)$ in correlation with $\text{BR}(H \rightarrow b\bar{b})$.

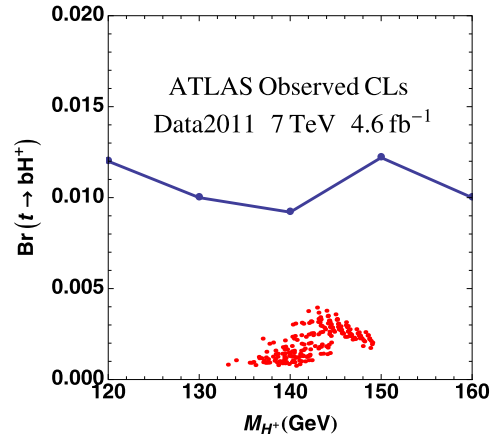


Fig. 4. $\text{BR}(t \rightarrow bH^\pm)$ vs M_{H^\pm} by assuming $\text{BR}(H^+ \rightarrow \tau^+\nu_\tau) = 100\%$. Red dots are parameter points that pass all our selection and constraints. (For interpretation of the references to color in this figure legend, the reader is referred to the web version of this Letter.)

into the $4b$, 4τ or $2b2\tau$ channels. The phenomenology of such channels has been widely studied in the context of NMSSM with $h \rightarrow AA$ search [40]. Studies of $h \rightarrow AA$ in NMSSM show that for $M_h \sim 120$ GeV, it requires the 14 TeV LHC with at least 100 fb^{-1} of data to claim discovery. Therefore, we argue the $H \rightarrow hh$ decay is not constrained by any current direct search experimental data from LHC. In Fig. 3, all the points $R_{\tau\tau} < 1$ bare the same feature as $\text{BR}(H \rightarrow hh) \sim 50\%$. Among these points, predictions on WW^* and ZZ^* are also slightly higher than the SM values but mostly within 1.5 which is consistent with the experimental data. The current search of $H \rightarrow \tau\tau$ at ATLAS is still with large error bar and consistent with these large numbers of $2 \sigma_{\text{SM}}^{\tau\tau}$. However, CMS Collaboration has reported their latest data that exclude the SM $\tau\tau$ rate by 1σ [42]. If one takes this seriously, most of our final survival parameter region will be cut away and only a few points that with significant $H \rightarrow hh$ decay can survive. In addition, the $H \rightarrow b\bar{b}$ are highly suppressed in these points and the predictions of these points agree with ATLAS central values of R in all channels very well. In principle, the choice of M_A can be extended to $\mathcal{O}(200 \text{ GeV})$ in our study and the flavor bounds are less constrained for larger M_A . However, the larger M_A region corresponds to the enhanced $R_{\tau\tau}$ region. Only smaller M_A generates larger splitting between H and h which reduces $R_{\tau\tau}$. Therefore, we only focus on the region $M_A \lesssim 150 \text{ GeV}$.

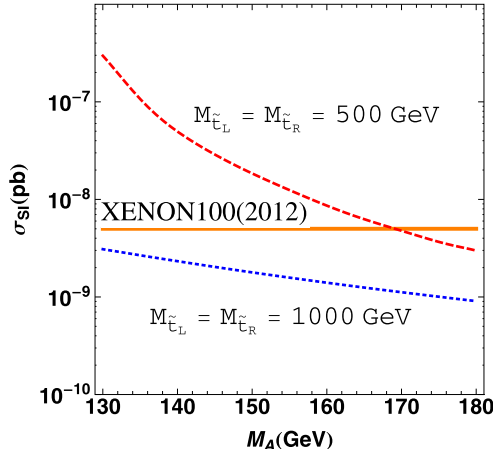


Fig. 5. Spin-independent scattering between neutralino dark matter and the nuclei computed for XENON100 by varying M_A . Red dashed line is in the case of light stop of 500 GeV and the blue dotted line corresponds to the stop mass of 1 TeV. (For interpretation of the references to color in this figure legend, the reader is referred to the web version of this Letter.)

Besides the direct search via $\tau\tau$, LHC has put much stronger bounds on $t \rightarrow bH^+$ with $H^+ \rightarrow \tau^+\nu_\tau$ comparing with Tevatron. The previous Tevatron upper bound of $\text{BR}(t \rightarrow bH^+)$ is 5% while the latest ATLAS results become 1–5%. We plot the $\text{BR}(t \rightarrow bH^+)$ with respect to M_{H^\pm} by assuming $\text{BR}(H^+ \rightarrow \tau^+\nu_\tau) = 100\%$ in Fig. 4. It clearly shows that all the parameter points that pass our selections are below the search of light charged Higgs boson via top decay $t \rightarrow bH^+$ with $H^+ \rightarrow \tau^+\nu_\tau$.

2.3. $\sigma_{\chi N}$

Finally we discuss the last constraint for non-decoupling MSSM. Latest direct dark matter detection experiments XENON100 have reached the level of sensitivity needed to detect neutralino dark matter over a substantial range of supersymmetric parameter space. These experiments attempt to detect weakly interacting (WIMP) dark matter particles through their elastic scattering with nuclei. Neutralinos can scatter with nuclei through both scalar (spin-independent) and axial-vector (spin-dependent) interactions. The experimental sensitivity to scalar couplings benefits from coherent scattering, which leads to cross sections and rates proportional to the square of the atomic mass of the target nuclei which is exactly being used for direct detection experiments. Consequently the spin-independent interactions are far more important than the spin-dependent in these experiments. In MSSM, the spin-independent interactions are mediated by the light Higgs bosons with cross section proportional to

$$\frac{\tan^2 \beta}{M_A^4}. \quad (16)$$

Fig. 5 has shown the spin-independent scattering between neutralino dark matter and the nuclei computed for XENON100 setup by varying M_A for pure-bino of 200 GeV to illustrate the enhancement feature due to light Higgs bosons and light top squarks. The calculation is done using *micrOMEGAs 2.4* [43]. It clearly shows the enhancement of such interaction in small M_A . In addition, squark can induce neutralino–gluon scattering which can further enhance the scattering cross section [44]. The two lines for different stop mass choices of 500 GeV and 1 TeV also indicate the enhancement of light stop in the neutralino–nuclei scattering. For most of our points with 500 GeV stop and $M_A \lesssim 170$ GeV, XENON100 bounds have put stringent constraints over the scenario. On the

other hand, it is not clearly whether the current dark matter completely consists of supersymmetric neutralino. The bounds can also be easily evaded by adding new component of dark matter from non-supersymmetric origin.

3. Conclusions

In this Letter, we discuss the non-decoupling MSSM scenario where a light Higgs boson can evade the direct search experiments at LEP or Tevatron and the 125 GeV Higgs-like boson is explained as the heavy Higgs boson in the spectrum. The light Higgs boson may evade the direct search experiments at LEP2 or Tevatron while the 125 GeV Higgs-like boson is identified as the heavy Higgs boson in the spectrum. Two direct consequences of the scenario are the flavor violation induced by the light charged scalar and the spin-independent scattering between neutralino and nuclei in dark matter direct detection experiments. With combined flavor constraints $B \rightarrow X_s \gamma$ and $B_s \rightarrow \mu^+ \mu^-$ and direct constraints on Higgs properties, we find best fit scenarios with light stop of $\mathcal{O}(500$ GeV), negative A_t around -750 GeV and large μ -term of 2–3 TeV. However, large parameter region in the survival space under all bounds may be further constrained by $H \rightarrow \tau\tau$ if no excess of $\tau\tau$ is confirmed at LHC. We only identify a small parameter region with significant $H \rightarrow hh$ decay that is consistent with all bounds and reduced $\tau\tau$ decay. In addition, if current dark matter mostly consists of neutralino, direct detection experiments like XENON100 also puts stringent bound over this scenario with light Higgs bosons. The light stops which are required by flavor constraints can further enhance the scattering cross section.

Note added in proof

When completing our work, arXiv:1211.1955 [hep-ph] [45] has appeared. The paper also studied similar region of non-decoupling MSSM and the results are in agreement with ours. We also include study on its enhancement of spin-independent neutralino–nuclei scattering. In addition, we find new parameter region which corresponds to reduce $R_{\tau\tau}$ due to $H \rightarrow hh$ decay.

Acknowledgements

ML is supported by the National Science Foundation of China (11135006) and National Basic Research Program of China (2010CB833000). KW is supported in part, by the Zhejiang University Fundamental Research Funds for the Central Universities (2011QNA3017) and the National Science Foundation of China (11245002, 11275168). GZ is supported in part, by the National Science Foundation of China (11075139, 11135006) and Program for New Century Excellent Talents in University.

References

- [1] G. Aad, et al., ATLAS Collaboration, *Phys. Lett. B* 716 (2012) 1, arXiv:1207.7214 [hep-ex]; S. Chatrchyan, et al., CMS Collaboration, *Phys. Lett. B* 716 (2012) 30, arXiv:1207.7235 [hep-ex].
- [2] ATLAS Collaboration, ATLAS-CONF-2012-098.
- [3] CDF Collaboration, arXiv:1207.0449 [hep-ex]; V.M. Abazov, et al., D0 Collaboration, arXiv:1207.0422 [hep-ex].
- [4] M. Carena, S. Gori, N.R. Shah, C.E.M. Wagner, *JHEP* 1203 (2012) 014, arXiv:1112.3336 [hep-ph]; M. Carena, S. Gori, N.R. Shah, C.E.M. Wagner, L.-T. Wang, *JHEP* 1207 (2012) 175, arXiv:1205.5842 [hep-ph]; J. Ke, M.-X. Luo, L.-Y. Shan, K. Wang, L. Wang, arXiv:1207.0990 [hep-ph].
- [5] M.R. Buckley, D. Hooper, arXiv:1207.1445 [hep-ph].
- [6] A. Belyaev, Q.-H. Cao, D. Nomura, K. Tobe, C.-P. Yuan, *Phys. Rev. Lett.* 100 (2008) 061801, arXiv:hep-ph/0609079.
- [7] S. Heinemeyer, O. Stal, G. Weiglein, *Phys. Lett. B* 710 (2012) 201, arXiv:1112.3026 [hep-ph].

- [8] A. Bottino, N. Fornengo, S. Scopel, Phys. Rev. D 85 (2012) 095013, arXiv:1112.5666 [hep-ph].
- [9] N.D. Christensen, T. Han, S. Su, Phys. Rev. D 85 (2012) 115018, arXiv:1203.3207 [hep-ph].
- [10] K. Hagiwara, J.S. Lee, J. Nakamura, arXiv:1207.0802 [hep-ph].
- [11] R. Benbrik, M.G. Bock, S. Heinemeyer, O. Stal, G. Weiglein, L. Zeune, arXiv:1207.1096 [hep-ph].
- [12] A. Arbey, M. Battaglia, A. Djouadi, F. Mahmoudi, JHEP 1209 (2012) 107, arXiv:1207.1348 [hep-ph].
- [13] G. Belanger, U. Ellwanger, J.F. Gunion, Y. Jiang, S. Kraml, J.H. Schwarz, arXiv:1210.1976 [hep-ph].
- [14] M. Drees, arXiv:1210.6507 [hep-ph].
- [15] LEP Higgs Working Group for Higgs boson searches, ALEPH Collaboration, DELPHI Collaboration, L3 Collaboration, OPAL Collaboration, arXiv:hep-ex/0107031.
- [16] G. Aad, et al., ATLAS Collaboration, JHEP 1206 (2012) 039, arXiv:1204.2760 [hep-ex].
- [17] U. Haisch, F. Mahmoudi, arXiv:1210.7806 [hep-ph].
- [18] W.-S. Hou, Phys. Rev. D 48 (1993) 2342.
- [19] A.G. Akeroyd, S. Recksiegel, J. Phys. G 29 (2003) 2311, arXiv:hep-ph/0306037.
- [20] G. Isidori, P. Paradisi, Phys. Lett. B 639 (2006) 499, arXiv:hep-ph/0605012.
- [21] Y. Amhis, et al., Heavy Flavor Averaging Group Collaboration, arXiv:1207.1158 [hep-ex], and online update at <http://www.slac.stanford.edu/xorg/hfag>.
- [22] M. Nakao, talk presented at 36th International Conference on High Energy Physics, Melbourne, 4–11 July, 2012.
- [23] J.-J. Cao, Z.-X. Heng, J.M. Yang, Y.-M. Zhang, J.-Y. Zhu, JHEP 1203 (2012) 086, arXiv:1202.5821 [hep-ph].
- [24] M.A. Ajaib, I. Gogoladze, Q. Shafi, arXiv:1207.7068 [hep-ph].
- [25] J. Hisano, S. Sugiyama, M. Yamanaka, M.J.S. Yang, Phys. Lett. B 694 (2011) 380, arXiv:1005.3648 [hep-ph].
- [26] E. Aprile, et al., XENON100 Collaboration, Phys. Rev. Lett. 109 (2012) 181301, arXiv:1207.5988 [astro-ph.CO].
- [27] M.S. Carena, D. Hooper, A. Vallinotto, Phys. Rev. D 75 (2007) 055010, arXiv:hep-ph/0611065.
- [28] M. Frank, T. Hahn, S. Heinemeyer, W. Hollik, H. Rzehak, G. Weiglein, JHEP 0702 (2007) 047, arXiv:hep-ph/0611326; G. Degrossi, S. Heinemeyer, W. Hollik, P. Slavich, G. Weiglein, Eur. Phys. J. C 28 (2003) 133, arXiv:hep-ph/0212020; S. Heinemeyer, W. Hollik, G. Weiglein, Eur. Phys. J. C 9 (1999) 343, arXiv:hep-ph/9812472; S. Heinemeyer, W. Hollik, G. Weiglein, Comput. Phys. Commun. 124 (2000) 76, arXiv:hep-ph/9812320.
- [29] P. Bechtle, O. Brein, S. Heinemeyer, G. Weiglein, K.E. Williams, Comput. Phys. Commun. 181 (2010) 138, arXiv:0811.4169 [hep-ph]; P. Bechtle, O. Brein, S. Heinemeyer, G. Weiglein, K.E. Williams, Comput. Phys. Commun. 182 (2011) 2605, arXiv:1102.1898 [hep-ph].
- [30] A. Crivellin, J. Rosiek, P.H. Chankowski, A. Dedes, S. Jaeger, P. Tanedo, arXiv:1203.5023 [hep-ph].
- [31] R. Barbieri, G.F. Giudice, Phys. Lett. B 309 (1993) 86, arXiv:hep-ph/9303270.
- [32] M.S. Carena, M. Olechowski, S. Pokorski, C.E.M. Wagner, Nucl. Phys. B 426 (1994) 269, arXiv:hep-ph/9402253.
- [33] M. Misiak, H.M. Asatrian, K. Bieri, M. Czakon, A. Czarnecki, T. Ewerth, A. Ferroglia, P. Gambino, et al., Phys. Rev. Lett. 98 (2007) 022002, arXiv:hep-ph/0609232.
- [34] A.J. Buras, J. Gierbach, D. Guadagnoli, G. Isidori, arXiv:1208.0934 [hep-ph].
- [35] CMS Collaboration, CMS-PAS-BPH-12-009.
- [36] K. De Bruyn, R. Fleischer, R. Kneijens, P. Koppenburg, M. Merk, N. Tuning, Phys. Rev. D 86 (2012) 014027, arXiv:1204.1735 [hep-ph].
- [37] K. De Bruyn, R. Fleischer, R. Kneijens, P. Koppenburg, M. Merk, A. Pellegrino, N. Tuning, Phys. Rev. Lett. 109 (2012) 041801, arXiv:1204.1737 [hep-ph].
- [38] A. Djouadi, Phys. Rept. 459 (2008) 1, arXiv:hep-ph/0503173.
- [39] M.S. Carena, J.R. Espinosa, M. Quiros, C.E.M. Wagner, Phys. Lett. B 355 (1995) 209, arXiv:hep-ph/9504316.
- [40] M. Carena, T. Han, G.-Y. Huang, C.E.M. Wagner, JHEP 0804 (2008) 092, arXiv:0712.2466 [hep-ph].
- [41] K.E. Williams, H. Rzehak, G. Weiglein, Eur. Phys. J. C 71 (2011) 1669, arXiv:1103.1335 [hep-ph]; K.E. Williams, G. Weiglein, Phys. Lett. B 660 (2008) 217, arXiv:0710.5320 [hep-ph].
- [42] CMS PAS HIG-12-018.
- [43] G. Bélanger, F. Boudjema, P. Brun, A. Pukhov, S. Rosier-Lees, P. Salati, A. Semenov, Comput. Phys. Commun. 182 (2011) 842, arXiv:1004.1092 [hep-ph].
- [44] M. Drees, M.M. Nojiri, Phys. Rev. D 47 (1993) 4226, arXiv:hep-ph/9210272.
- [45] P. Bechtle, S. Heinemeyer, O. Stal, T. Stefaniak, G. Weiglein, L. Zeune, arXiv:1211.1955 [hep-ph].